Available online at www.sciencedirect.com
ScienceDirect
Carbon 45 (2007) 3022–3026
CARBON
www.elsevier.com/locate/carbon

Graphene layers from thermal oxidation of exfoliated graphite plates

Z. Osváth [a,*], Al. Darabont [b], P. Nemes-Incze [a], E. Horváth [a], Z.E. Horváth [a], L.P. Biró [a]

[a] Research Institute for Technical Physics and Materials Science (MFA), H-1525 Budapest, P.O. Box 49, Hungary
[b] Faculty of Physics, "Babes-Bolyai" University, Strasse M. Kogalniceanu No. 1, R-3400, Cluj-Napoca, Romania

Received 18 June 2007; accepted 14 September 2007
Available online 21 September 2007

Abstract

Graphite platelets of 1–5 μm in diameter consisting of a few graphenes were generated from commercially available exfoliated graphite by ultrasonic treatment in benzene (1 mg material in 20 ml solvent) for 3 h. Droplets from the suspension were dispersed on silicon wafer. The graphite platelets were characterized by atomic force microscopy (AFM). Successive oxidation of the sample was carried out at 450–550 °C in air. AFM measurements showed that the thermal oxidation removed 2–3 graphenes from the platelets and it left behind single graphene layers.
© 2007 Published by Elsevier Ltd.

1. Introduction

Recently, graphene and few-layer graphite films received special interest from researchers active in the field of nanoscience. This interest is partly due to the remarkable electronic properties and ballistic transport properties of graphene layers [1–4], which make them suitable building blocks (beside carbon nanotubes) in many potential electronic applications. The first experimental graphene transistor has already been constructed [5]. It has been shown that the electronic properties of graphene ribbons depend on their width, because nanometer-sized widths induce the quantization of the allowed states [6,7], similar to the quantization of states induced by rolling a graphene sheet into a carbon nanotube. Furthermore, particular electronic states appear at the edges of graphene ribbons (edge effects), depending on the "zigzag" or "armchair" type edge terminations. The band structure of "zigzag" and "armchair" graphene ribbons have been investigated theoretically [8,9], and the corresponding edge states have been observed by scanning tunneling microscopy [10] and spectroscopy [11,12].

Graphene and few-layer graphite films were successfully produced by several methods. These methods include epitaxial growth on 6H- and 4H–SiC surface [7,13,14], micromechanical cleavage of highly oriented pyrolytic graphite (HOPG) followed by the identification and selection of monolayers using microscopy techniques [4,15,16], converting of diamond nanoparticles to single nanographenes by heat treatment at 1600 oC [17], growth of graphene layers on HOPG via exposure to methyl radicals generated by thermal decomposition of azomethane [18], and synthesis of few-layer graphite films by camphor pyrolysis on nickel substrates [19]. Graphitic nanoplatelets were also prepared via exfoliation/in-situ reduction of graphite oxide [20]. In this work we show that few-layer graphite platelets can be thinned by thermal oxidation in air, and individual graphene layers can be formed by this method.

2. Experimental

Commercial exfoliated graphite (1 mg material in 20 ml benzene) was treated ultrasonically for 3 h. Droplets from the suspension were dispersed on Si wafer. Graphite platelets of 1–5 μm in diameter were observed by tapping mode atomic force microscopy (AFM) using a Nanoscope IIIa instrument operating in air. After the AFM investigation, the sample was introduced into a quartz reactor of 18 mm inner diameter and oxidized in an electric furnace with an effective heating length of 200 mm [21]. The oxidation was carried out in three steps. In the first step the

* Corresponding author. Fax: +36 1 392 2226.
E-mail address: osvath@mfa.kfki.hu (Z. Osváth).

0008-6223/$ - see front matter © 2007 Published by Elsevier Ltd.
doi:10.1016/j.carbon.2007.09.033

sample was oxidized at 450 °C for 10 min (step I). In the second and the third steps the sample was heated at 550 °C for 10 min (step II) and 20 min (step III), respectively. AFM measurements were performed after each oxidation step and the effect of oxidation was observed on the same graphite platelet. This was achieved by placing markers on the Si substrate near the graphite platelet with focused ion beam (FIB) technique performed in a LEO 1540XB instrument. The markers guided us to find the graphite platelet by AFM after each oxidation step.

3. Results and discussion

The effect of oxidation was observed on several graphite platelets. Fig. 1 denotes the platelet on which the effect was investigated in more detail. The AFM image in Fig. 1a shows the graphite platelet before oxidation. It can be observed that the platelet folds in several places and a lot of nanoparticles stick to its surface. Most probably these particles are amorphous carbon or solvent residue attached to defect sites. We observed that after oxidation step I (450 °C for 10 min) the majority of the nanoparticles evaporated from the surface (see Fig. 1b). The surface roughness (RMS) of the platelet (measured in the center) decreased from 1.4 nm (before oxidation) to 0.25 nm after the oxidation step I, while the roughness of the Si substrate did not change (0.1 nm). Furthermore, the measurements show that the graphite platelet flattened and could fit better to the substrate. This shows that the residue material evaporated not only from the surface, but also from the space between the platelet and the Si substrate (the interface was cleaned).

Due to this flattening the height of the platelet could be measured more accurately. The height of this platelet measured at its central part is 2.7 nm, which most probably corresponds to 8 graphene layers separated by the 0.34 nm Van der Waals distance. We can observe in Fig. 1b that it is not just one platelet that we are measuring, but there are at least three smaller graphite platelets which fold several times and intersect each other. This could be better observed after the first oxidation step (heat treatment), when the platelets were smoothed out.

To study in more detail the effect of oxidation, we selected an area near the right-hand side edge of the platelet, denoted by small boxes in Fig. 1. This portion of the graphite platelet is shown in Fig. 2 before oxidation (Fig. 2a), and after the oxidation steps I (Fig. 2b), II (Fig. 2c), and III (Fig. 2d). One can observe that the height of this part of the platelet which was 2.9 nm before oxidation (Fig. 2a) decreased to 0.7–1.1 nm after the oxidation step I (Fig. 2b). As we mentioned earlier, this decrease is not due to removal of graphene layers but to the removal of residue material, and this induces the flattening of the graphite platelet. The label marks 11′ in Fig. 2b show a height of 0.7 nm, which corresponds to the thickness of two graphene layers. However, we can easily notice that the platelet thickness is not uniform. The marks labeled 22′ show thicker parts with 0.37 nm additional height, which is due to the presence of another incomplete graphene layer. One can observe several pits on the surface in Fig. 2b, at the regions where this top graphene layer is missing. One can say that the original platelet had a thickness of 3 graphene layers (~1.1 nm in height), and monolayer deep pits started to appear in the top layer due to the oxidation step I. Graphite is a relatively inert material, but it was shown that it oxidizes at temperatures >400 °C in oxygen [22,23], and the oxidation occurs predominantly at the edges and defect sites [24–26]. Similar oxidation pits were observed by scanning tunneling microscopy on oxidized highly oriented pyrolitic graphite (HOPG) surfaces [27–29].

Fig. 2c shows the graphite platelet after oxidation step II (550 °C for 10 min). One can observe that in this case the

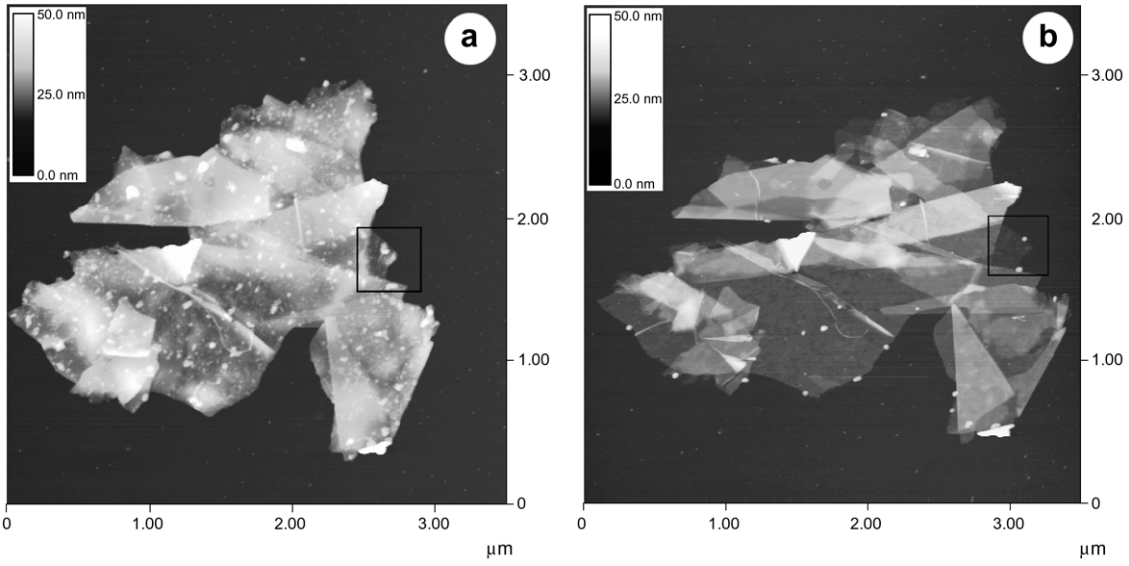

Fig. 1. AFM images of a few-layer graphite platelet: (a) before oxidation and (b) after the first oxidation step (450 °C in air for 10 min). The small boxes indicate the part of the platelet which is detailed in Fig. 2.

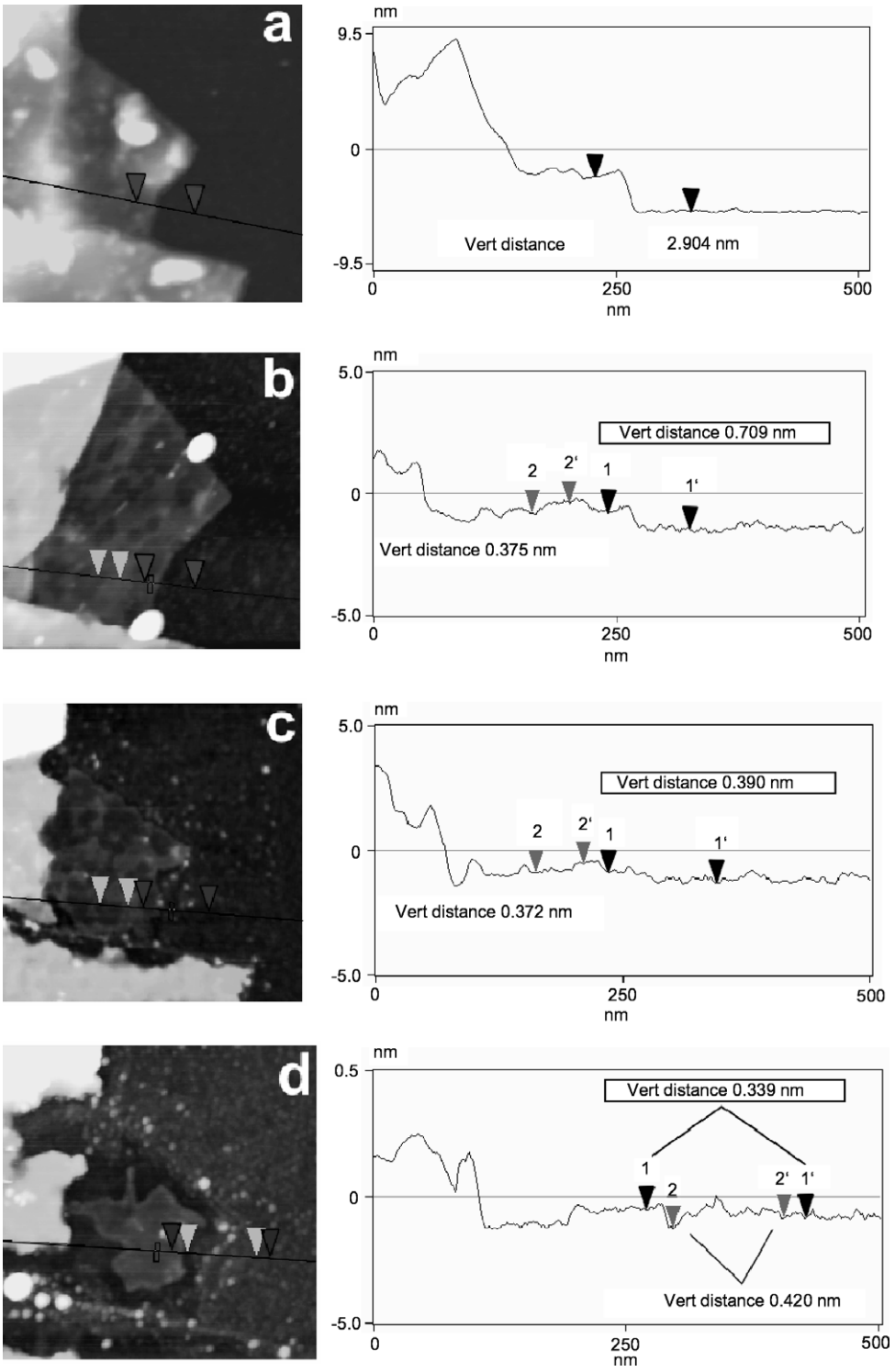

Fig. 2. AFM images of the same area of the few-layer graphite platelet showing the effect of oxidation: (a) before oxidation; (b) after oxidation step I (450 °C for 10 min); (c) after oxidation step II (550 °C for 10 min); and (d) after oxidation step III (550 °C for 20 min).

platelet edges have also been oxidized and the shape of the analyzed area has changed. The label marks 11′ show a height of 0.39 nm, which means that the thickness of this part has been decreased to one graphene layer. Similarly to Fig. 2b, the platelet thickness is not uniform, the label marks 22′ show two-layer thick islands. The effect of the third oxidation step (550 °C for 20 min) is illustrated in Fig. 2d. Notice that the thickness of the platelet became uniform, the islands of the second layer were removed completely and eventually we obtained a single graphene layer (label marks 11′). The oxidation decreased also the horizontal diameters of the platelet. As a consequence, the

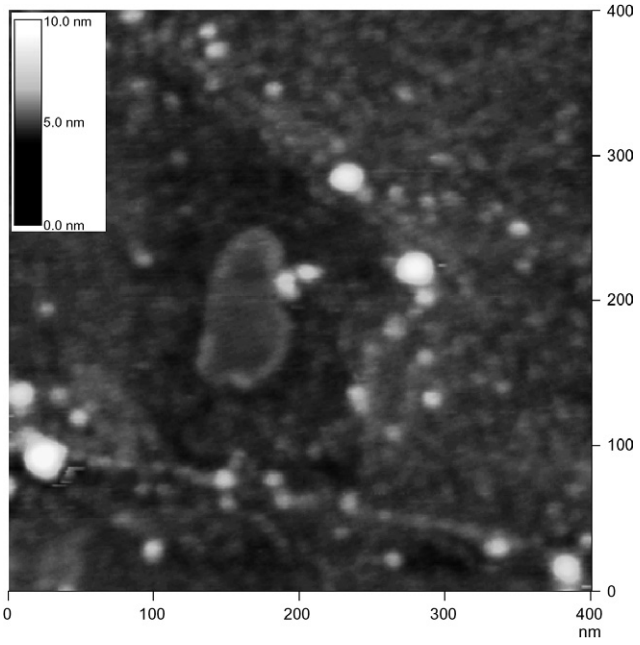

Fig. 3. AFM image of a 105 nm long and 51 nm wide graphene ribbon (center of figure), which was created during the forth oxidation step (550 °C for 30 min).

analyzed part detached from the body platelet and it can be considered a standalone graphene layer (Fig. 2d). One can observe that the substrate surface (the native SiO_2 layer) has also been etched, and approx. 0.4 nm deep trenches have formed along the circumference of the graphene platelet (label marks 22′). This effect was also demonstrated in a recent work, where the formation of SiO_2 nanotrenches was guided by carbon nanotubes dispersed on the surface [30].

The shape of the obtained graphene platelet is quite irregular (Fig. 2d), which is somewhat expectable because the oxidation is not uniform, even in the case of very small areas [27]. However, the oxidation pits observed earlier on HOPG surfaces can be very regular [29]. For example, hexagonal pits with armchair edges can easily form, because armchair edges are less reactive [28]. Considering this, we decided to perform a forth oxidation step. We wanted to observe whether the graphene platelet shown in Fig. 2d was going to develop a more regular shape or not, as its diameter further decreases due to oxidation. This forth oxidation step was done at 550 °C for 30 min. The AFM image of the graphene platelet after this oxidation step is presented in Fig. 3. One can observe that only a 105 nm long and 51 nm wide graphene ribbon has been left from the platelet (see center of Fig. 3).

Although it does not have a specific regular shape, it is worthy to note that the left side edge of the platelet follows a straight line and it is probably an armchair edge (which is more resistant to oxidation [28]). Further oxidation steps would probably remove the graphene ribbon completely. The above results show that thermal oxidation does not produce graphene ribbons with very regular shapes, although the method can be used to reduce the dimensions of graphene platelets. Accordingly, the reduced dimensions can change the electronic properties of the platelets due to electronic confinement [6,7].

4. Conclusions

Graphite platelets consisting of a few graphenes were characterized by AFM. Successive oxidation of the platelets was carried out at 450–550 °C in air. AFM measurements were performed after each oxidation step and the effect of oxidation was observed. The measurements showed that the thermal oxidation removed 2–3 graphenes from the platelets and created individual graphene layers. We showed that this oxidation procedure could be applied to decrease the thickness of graphite platelets.

Acknowledgements

This work has been done in the framework of the GDR-I No. 2756 (GDR on Science and Applications of Nanotubes – NANO-E). The authors acknowledge the financial support from OTKA K49182, OTKA-NKTH K67793, and NKTH "MOFENACS".

References

[1] Frank S, Poncharal P, Wang Z, de Heer WA. Carbon nanotube quantum resistors. Science 1998;280:1744–6.
[2] Liang W, Bockrath M, Bozovic D, Hafner J, Tinkham M, Park H. Fabry-Perot interference in a nanotube electron waveguide. Nature 2001;411:665–9.
[3] Poncharal P, Berger C, Yi Y, Wang Z, de Heer W. Room temperature ballistic conduction in carbon nanotubes. J Phys Chem B 2002;106:12104–18.
[4] Novoselov KS, Geim AK, Morozov SV, Jiang D, Zhang Y, Dubonos SV, et al. Electric field effect in atomically thin carbon films. Science 2004;306:666–9.
[5] Lemme MC, Echtermeyer TJ, Baus M, Kurz H. A graphene field-effect device. IEEE Electro Dev Lett 2007;28:282–4.
[6] Barone V, Hod O, Scuseria GE. Electronic structure and stability of semiconducting graphene nanoribbons. Nano Lett 2006;6:2748–54.
[7] Berger C, Song Z, Li X, Wu X, Brown N, Naud C, et al. Electronic confinement and coherence in patterned epitaxial graphene. Science 2006;312:1191–6.
[8] Nakada K, Fujita M, Dresselhaus G, Dresselhaus MS. Edge state in graphene ribbons: nanometer size effect and edge shape dependence. Phys Rev B 1996;54:17954–61.
[9] Wakabayashi K. Electronic transport properties of nanographite ribbon junctions. Phys Rev B 2001;64:125428(15).
[10] Giunta PL, Kelty SP. Direct observation of graphite layer edge states by scanning tunneling microscopy. J Chem Phys 2001;114:1807–12.
[11] Niimi Y, Matsui T, Kambara H, Tagami K, Tsukada M, Fukuyama H. Scanning tunneling microscopy and spectroscopy studies of graphite edges. Appl Surf Sci 2005;241:43–8.
[12] Niimi Y, Matsui T, Kambara H, Tagami K, Tsukada M, Fukuyama H. Scanning tunneling microscopy and spectroscopy of the electronic local density of states of graphite surfaces near monoatomic step edges. Phys Rev B 2006;73:085421(8).
[13] Berger C, Song Z, Li T, Li X, Ogbazghi AY, Feng R, et al. Ultrathin epitaxial graphite: 2D electron gas properties and a route toward graphene-based nanoelectronics. J Phys Chem B 2004;108:19912–6.

[14] Hass J, Feng R, Li T, Li X, Zong Z, de Heer WA, et al. Highly ordered graphene for two-dimensional electronics. Appl Phys Lett 2006;89:143106(3).
[15] Lu X, Huang H, Nemchuk N, Ruoff RS. Patterning of highly oriented pyrolytic graphite by oxygen plasma etching. Appl Phys Lett 1999;75:193–5.
[16] Novoselov KS, Geim AK, Morozov SV, Jiang D, Katsnelson MI, Grigorieva IV, et al. Two-dimensional gas of massless dirac fermions in graphene. Nature 2005;438:197–200.
[17] Affoune AM, Prasad BLV, Sato H, Enoki T, Kaburagi Y, Hishiyama Y. Experimental evidence of a single nanographene. Chem Phys Lett 2001;348:17–20.
[18] Wellmann R, Böttcher A, Kappes M, Kohl U, Niehus H. Growth of graphene layers on HOPG via exposure to methyl radicals. Surf Sci 2003;542:81–93.
[19] Somani PR, Somani SP, Umeno M. Planer nanographenes from camphor by CVD. Chem Phys Lett 2006;430:56–9.
[20] Stankovich S, Piner RD, Chen X, Wu N, Nguyen ST, Ruoff RS. Stable aqueous dispersions of graphitic nanoplatelets via the reduction of exfoliated graphite oxide in the presence of poly(sodium 4-styrenesulfonate). J Mater Chem 2006;16:155–8.
[21] Tapasztó L, Kertész K, Vértesy Z, Horváth ZE, Koós AA, Osváth Z, et al. Diameter and morphology dependence on experimental conditions carbon nanotube arrays grown by spray pyrolysis. Carbon 2005;43:970–7.
[22] Marsh H. Introduction to carbon science. London: Butterworths; 1989.
[23] Blackman LCF. Modern aspects of graphite technology. London: Academic Press; 1970.
[24] Hennig GR. In: Walker Jr PL, editor. Chemistry and physics of carbon, vol. 2. New York: Marcel Dekker; 1966. p. 1.
[25] Thomas JM. In: Walker Jr PL, editor. Chemistry and physics of carbon, vol. 1. New York: Marcel Dekker; 1965. p. 121.
[26] Ergun S, Menster M. In: Walker Jr PL, editor. Chemistry and physics of carbon, vol. 1. New York: Marcel Dekker; 1965. p. 203.
[27] Klusek Z. Scanning tunneling microscopy and spectroscopy of the thermally oxidized (0001) basal plane of highly oriented pyrolitic graphite. Appl Surf Sci 1998;125:339–50.
[28] Tandon D, Hippo EJ, Marsh H, Sebok E. Surface topography of oxidized HOPG by scanning tunneling microscopy. Carbon 1997;35:35–44.
[29] Zhang WG, Cheng HM, Xie TS, Shen ZH, Zhou BL, Ye HQ. STM observation of oxidation morphology of HOPG and boron-doped HOPG. Carbon 1997;35:1839–41.
[30] Byon HR, Choi HC. Carbon nanotube guided formation of silicon oxide nanotrenches. Nat Nanotechnol 2007;2:162–6.